Available online at www.sciencedirect.com
ScienceDirect
Carbohydrate Polymers 73 (2008) 390–400
Carbohydrate Polymers
www.elsevier.com/locate/carbpol

Novel super pH-sensitive nanoparticles responsive to tumor extracellular pH

Li Fan [a], Hong Wu [a,*], Hui Zhang [a], Fei Li [a], Tie-hong Yang [b], Chun-hu Gu [c], Qian Yang [d]

[a] Department of Chemistry, School of Pharmacy, Fourth Military Medical University, Xi'an 710032, China
[b] Department of Pharmacology, School of Pharmacy, Fourth Military Medical University, Xi'an 710032, China
[c] Xijing Hospital, Fourth Military Medical University, Xi'an 710032, China
[d] Institute of Pharmaceutical Research, School of Pharmacy, Fourth Military Medical University, Xi'an 710032, China

Received 13 September 2007; received in revised form 5 December 2007; accepted 5 December 2007
Available online 21 February 2008

Abstract

The objective of this study was to evaluate Camptothecin (CAMP)-loaded poly(*N*-isopropylacrylamide) (NIPAAm)/chitosan nanoparticles as a pH-sensitive carrier for specifically targeting tumors. The synthesis and properties of the system was studied by adjusting the mass ratio of NIPAAm and chitosan. The drug release characteristics of nanoparticles in vitro were investigated. The results showed that when the charge ratio between NIPAAm and chitosan of 4:1 (w/w) was achieved, the drug-loaded nanoparticles were most sensitive to tumor pH. Encapsulation efficiencies and loading were 73.7% and 8.4%, respectively. The cumulative release rate of CAMP was optimal at pH 6.8 and decreased rapidly either below pH 6.5 or above pH 6.9 in 37 °C. Based on MTT (3-(4,5-dimethylthiazol-2-yl)-2,5-diphenyltetrazolium) test and fluorescence microscopy results, CAMP-loaded nanoparticles showed cytotoxicity at pH 6.8 but minimal cytotoxicity at pH 7.4. The pH-sensitive poly NIPAAm/chitosan nanoparticles provided some distinct advantages in delivering anti-cancer drugs to targeted tissues.

Keywords: NIPAAm; Chitosan; CAMP; Tumor pH; pH-sensitivity

1. Introduction

It is well known that most chemotherapy drugs are taken up non-specifically by all types of cells resulting in serious side effects. Therefore, an ideal carrier for delivering drugs for cancer treatment should be able to transport the drug specifically to the tumor region before it is released. One of the consistent differences between various solid tumors and the surrounding normal tissue is their chemical and metabolic environment (Conner, Yatvin, & Huang, 1984; Stubbs, McSheehy, Griffiths, & Bashford, 2000; Tannock & Rotin, 1989). Most solid tumors have lower extracellular pH (<7.2) than the surrounding tissues and blood (pH 7.5) (Langerman et al., 1990; Stubbs et al., 2000). In addition, the temperature around tumor cells is about 0.5 °C higher than the surrounding normal tissue because of intratumoral prosperity metabolism (Yahara et al., 2003). Based on these differences, an ideal drug delivery system would possess the ability to switch from no-release in normal healthy tissue to a fast-release at the tumor site.

In recent years, stimuli-sensitive polymers have been proposed as new anti-cancer drug carriers because such polymeric nanoparticles can alter their physical properties in response to the changes in external stimuli such as pH (Kang & Bae, 2001), temperature (Katayama & Ohata, 1984), light (Suzuki & Tanaka, 1990), and metabolites (Cartier, Horbett, & Ratner, 1995). Among them, pH-sensitive polymers have attracted rapidly growing interest in both the biomedical and biotechnological fields (Benrebouh, Avoce, & Zhu, 2001; Chiu, Wu, & Lin, 2001; Kathmann, White, & McCormick, 1997; Ogawa, Ogawa, Wang, & Kokufuta, 2001; Sakata, Todokoro, Kai, Kunitake, & Hirayama, 2001; Yuk, Cho, & Lee, 1997).

* Corresponding author. Tel.: +86 29 84774473; fax: +86 29 84776945.
E-mail address: hongwuxa@hotmail.com (H. Wu).

0144-8617/$ - see front matter © 2007 Elsevier Ltd. All rights reserved.
doi:10.1016/j.carbpol.2007.12.006

There have been recent reports of the possibility of developing thermo-sensitive and pH-sensitive polymeric nanoparticles for targeting drug delivery to tumors, i.e., passive accumulation/aggregation as well as the enhanced release of drugs by an externally provided hyperthermic condition (Cammas et al., 1997; Chung, Yokoyama, & Okano, 2000; Kong, Braun, & Dewhirst, 2001), and pH-sensitive polymers as drug carriers by a definite phase-transition pH (Du, Dai, Liu, & Dankovich, 2006; Shu, Zhu, & Song, 2001).

Temperature sensitive polymeric micelles composed of a hydrophobic core and a temperature sensitive shell and micelle aggregation as well as an enhanced release rate of the loaded drug was reported by Okano et al. (Chung et al., 1999, 2000; Yokoyama & Okano, 1996). A synergistic effect was expected between chemotherapy and hyperthermic treatment of tumor cells at 42 °C. However, this approach was difficult to administer because of the need for an external supply of heat. It was also difficult to induce a hyperthermic condition in tumors unless they were located near the surface of the body.

The pH-induced transitions in polymer conformation, solubility and swelling mostly occur in the range of pH 4–6 for polymers with a weak acidic group and above pH 8 for those with a weak base group because of their intrinsic dissociation constants (p*K*). Some attempts to adjust the transition pH to neutral have been tried through the copolymerization of weak acidic or basic monomers (Feil, Bae, Feijen, & Kim, 1992; Philippova, Hourdet, Audebert, & Khokhlov, 1997). However, systems responsive to small fluctuations in pH at physiological condition are seldom observed. There is still a need for medical research to develop nanocarriers that are truly responsive to tumor pH for direct tumor targeting.

Poly(*N*-isopropylacrylamide) (PNIPAAm) is a well-known member of the thermo-responsive polymer family. Based upon its conformational changes, various PNIPAM hydrogels had been studied as controlled optical switches, limiters and modulators (Wang, Fang, & Hu, 2001). Even more, *N*-isopropylacrylamide (NIPAAm) was studied widely in its thermo responsive characteristic with potential use in drug targeting (Lin, Chiu, & Lee, 2005a). Recently, thermo- and pH-sensitive hydrogels were prepared by graft copolymerization or interpenetrated networks of chitosan (CS) and NIPAAm to enhance loading capacity and controlled release properties (Alvarez-Lorenzo et al., 2005; Cai, Zhang, Sun, He, & Zhu, 2005; Lin, Chiu, & Lee, 2005b).

In this paper, we present novel super pH-sensitive nanoparticles based on graft copolymerization of NIPAAm and chitosan as a delivery system for an anti-tumor drug, CAMP. CAMP is an alkaloid that shows strong cytotoxic activity against various cancer cell lines. It has been effective in the treatment of colorectal cancer and ovarian cancer (Chris, John, & Susan, 1998; Subrahmanyam et al., 1998). CAMP treatment has been limited due to side effects (Moertel, Schutt, Reitemeier, & Hahn, 1972; Muggia, Creaven, Hansen, Cohen, & Sealwry, 1972). However, side effects from CAMP can be minimized by delivering the drug only to the tumor tissue. The purpose of the present study was to develop a pH-sensitive drug delivery system which releases CAMP into tumor tissue with little or no release in normal tissue.

2. Experimental

2.1. Materials

NIPAAm (Sigma–Aldrich) was purified by repeated recrystallization in a mixture of toluene and hexane (1:5 v/v), giving spindle-like crystals. Chitosan (medium, Mw: approximate 75,000, degree of deacetylation: 74%), the cross-linker *N*,*N*-methylene-bisacrylamide (MBA), initiator *tert*-butyl hydroperoxide (TBHP, 70% solution in water) and ammonium persulfate (APS), the accelerator *N*,*N*,*N*′,*N*′-tetramethyl-ethylenediamine (TEMED), surfactants sodium dodecylsulfate (SDS), dodecyl-trimethylammonium bromide (DTAB), and CAMP with purity exceeding 99% were all purchased from Aldrich Chemical Co. Freshly deionized and distilled water was used as the dispersion medium.

2.2. Methods

2.2.1. Preparation of poly NIPAAm/chitosan and PNIPAAm nanoparticles

To obtain poly NIPAAm/chitosan nanoparticles, for a total solution of 50 mL, chitosan (0.25 g) was first dissolved in a 5% acetic acid solution. A mixture of purified NIPAAm monomer (1.0 g) and MBA (0.01 g) was charged to the chitosan solution and mixed in a water-jacketed flask equipped with a thermometer, a condenser, a magnetic stirrer, and a nitrogen inlet under nitrogen for 30 min at 70 °C. Dilute TBHP solution (0.8 mL, 1.0×10^{-2} M) was added dropwise to the mixture, and the solution was stirred at 70 °C for 3 h under nitrogen. The dispersion of nanoparticles was carefully purified by repeated centrifugation at 13,000 rpm for 30 min and decantation until the conductivity of the supernatant was close to that of the water used. The dispersion was further purified by placing it into a dialysis tube with a 100,000 Da molecular weight cut-off (Spectria/Por®CE) and dialyzed against 1 L of water for one week at room temperature with daily changing of water. The nanoparticles were then lyophilized and stored at 4 °C before further study.

PNIPAAm nanoparticles were synthesized by free-radical emulsion polymerization of NIPAAm in aqueous solutions. APS (0.05 M) and TEMED (0.32 M) were used as the redox initiator system. The amount of MBA in the monomer mixture was 0.5 wt% (m/m). The NIPAAm (1 g), APS (1.0 mL) and MBA (5 mg) were dissolved in distilled water (4 mL) under stirring and the solution was purged with nitrogen gas for 30 min.

After the addition of TEMED (0.5 mL), the solution was stirred in a thermostated water bath at 30 °C, and the polymerization was conducted for 24 h. Upon completion of the reaction, the solution was further purified by placing it into a dialysis tube with a 100,000 Da molecular weight cut-off (Spectria/Por®CE) and dialyzed in large excess of water to wash out any unreacted monomers and the initiator. The nanoparticles were then lyophilized and stored at 4 °C. To remove the homopolymer of NIPAAm, the products were followed by soxhlet extraction with methanol for 48 h. The resulting products were dried under atmosphere for 24 h and then in vacuo at 30 °C for 24 h.

The percentage of grafting (%) was calculated by the difference of weights before and after grafting reaction according to the following formula:

$$\text{Percentage of grafting } (\%) = \frac{W_f - W_c}{W_c} \times 100,$$

where W_f, and W_c denote the weight of final product (chitosan-g-NIPAAm), and initial chitosan charged, respectively.

2.2.2. Fourier transform infrared and ^{1}H-NMR spectroscopy measurements

Fourier transform infrared (FTIR, Thermo Nicolet Avetar 370, USA) and ^{1}H-nuclear magnetic resonance (^{1}H-NMR, Bruker AMX-500) measurements were used to investigate the chemical structure of chitosan-g-NIPAAm.

2.2.3. Preparation of CAMP-loaded poly NIPAAm/chitosan and PNIPAAm

2.2.3.1. Nanoparticles. The procedure of CAMP loaded poly NIPAAm/chitosan and PNIPAAm nanoparticles was similar to that of blank nanoparticles with initially adding 200 mg CAMP into the solution. The nanoparticles were collected by centrifugation and washed four times with distilled water. The nanoparticles were then lyophilized and stored at 4 °C.

2.2.4. Transmission electron microscopy (TEM) examinations

A drop of the resultant nanoparticles solution containing 0.01 (w/v)% phosphotungstic acid was placed on a copper grid coated with carbon film, and air-dried at 20 °C. The TEM observations were carried out on a JEM-2010 microscope (Japan) with an electron kinetic energy of 300 keV.

2.2.5. Measurement of size and stability of nanoparticles

Size of all blank and drug loaded samples were measured by photon correlation spectroscopy using Zetasizer 3000 HAS (Malvern Instruments, UK). All the samples were diluted with aqueous phase of the formulation to get optimum kilo counts per second (kcps) of 50–200 for measurements. The collected nanoparticles were sealed and deposited in a 4 °C refrigerator or at room temperature in a desiccator for three months, respectively. The appearance, morphology and drug content of nanoparticles were tested.

2.2.6. Determination of encapsulation efficiencies and loading

An exactly weighed amount of drug-loaded nanoparticles suspension (200 mg) was hydrolyzed in 1 M HCl at 60 °C water bath for 1 h up to the solution become clarification and membrane filtration. The mixture containing the drug was determined using high-performance liquid chromatography (HPLC) system. The HPLC assay (Agilent 1100 series) for CAMP was performed on a reverse phase Techsphere ODS column (25 cm × 4.6 mm ID, 5 μm). The mobile phase was set as acetonitrile:water, 4:6 and separation was carried out at a flow rate of 1.0 mL/min. The compounds were detected using a UV detector at λ_{max} of 254 nm. The standard curve for the quantification for CAMP was linear over the range of standard concentration between 50 and 100,000 ng/mL with a correlation coefficient of $R^2 = 0.999$. Loading efficiency and encapsulation efficiency were calculated as following:

$$\text{Encapsulation efficiency } (\%) = \frac{\text{Weight of drug found loaded}}{\text{Weight of drug input}} \times 100,$$

$$\text{Loading efficiency } (\%) = \frac{\text{Weight of drug found loaded}}{\text{Weight of drug} - \text{loaded nanoparticles}} \times 100.$$

2.2.7. pH and temperature-sensitive characteristics

In vitro pH-sensitive drug release profiles were obtained by a dynamic dialysis method. The release experiments were conducted at 37 °C. Typically, 0.2 g of CAMP-loaded nanoparticles were placed into a dialysis bag, respectively, and introduced to 100 mL of phosphate-buffered solution (PBS, pH 5.0–8.0), respectively, with magnetically stirring at 200 rpm. At hourly intervals, 3 mL of samples were removed from the release medium and the same volume and temperature of PBS was added to the release medium. Then the samples were assayed for drug content according to the standard curve. Results of triplicate tests data were used to calculate accumulated drug release.

In vitro temperature sensitive drug release profiles were obtained the same dynamic dialysis method above which was conducted at pH 6.8 phosphate-buffered solution at temperature range from 25 to 40 °C, respectively.

2.2.8. In vitro cytotoxicity measurement of blank nanoparticles and pH-sensitive cytotoxicity measurement of drug loaded nanoparticles

2.2.8.1. Cell culture. Human colon carcinoma cells SW480 and human fibroblast were cultured in a RPMI 1640 medium with 2 mM L-glutamine, 5% penicillin–streptomycin,

and 10% fetal bovine serum in a humidified incubator at 37 °C and with a 5% CO_2 atmosphere.

In vitro cytotoxicity of blank and drug loaded nanoparticles were measured using human fibroblast and human colon carcinoma cells SW480. The cells were plated at a density of 2×10^3 cells/well in 96-well tissue culture dishes cultured for 24 h and then exposed to blank nanoparticles for another 12 h. After nanoparticles exposure at various concentrations, the cells were washed three times with RPMI 1640 medium, and 200 μL of RPMI 1640 medium without serum were then added. Cytotoxicity was assessed using MTT to measure the viability of the cells. Fifty microliters of MTT solution (5 mg/mL) was added to each well. The plates were incubated for an additional 4 h and then the medium was discarded. One hundred fifty microliters of DMSO were added to each well, and the solution was vigorously mixed to dissolve the reacted dye. The absorbance of each well was read on a microplate reader (FL600, Bio-Tek, USA) at a test wavelength of 490 nm and a reference wavelength of 570 nm. In vitro pH-sensitive cytotoxicity measurement of drug loaded nanoparticles was the same with initially plating the cells at a density of 2×10^3 cells/well in 96-well tissue culture dishes for 24 h and then exposing them to free CAMP and CAMP-loaded nanoparticles for 48 h at pH 7.4 and 6.8, respectively.

2.2.9. RBITC-labeling of nanoparticles and fluorescence microscopic study

The procedure of preparing RBITC-labeling nanoparticles was similar to that of blank poly NIPAAm/chitosan

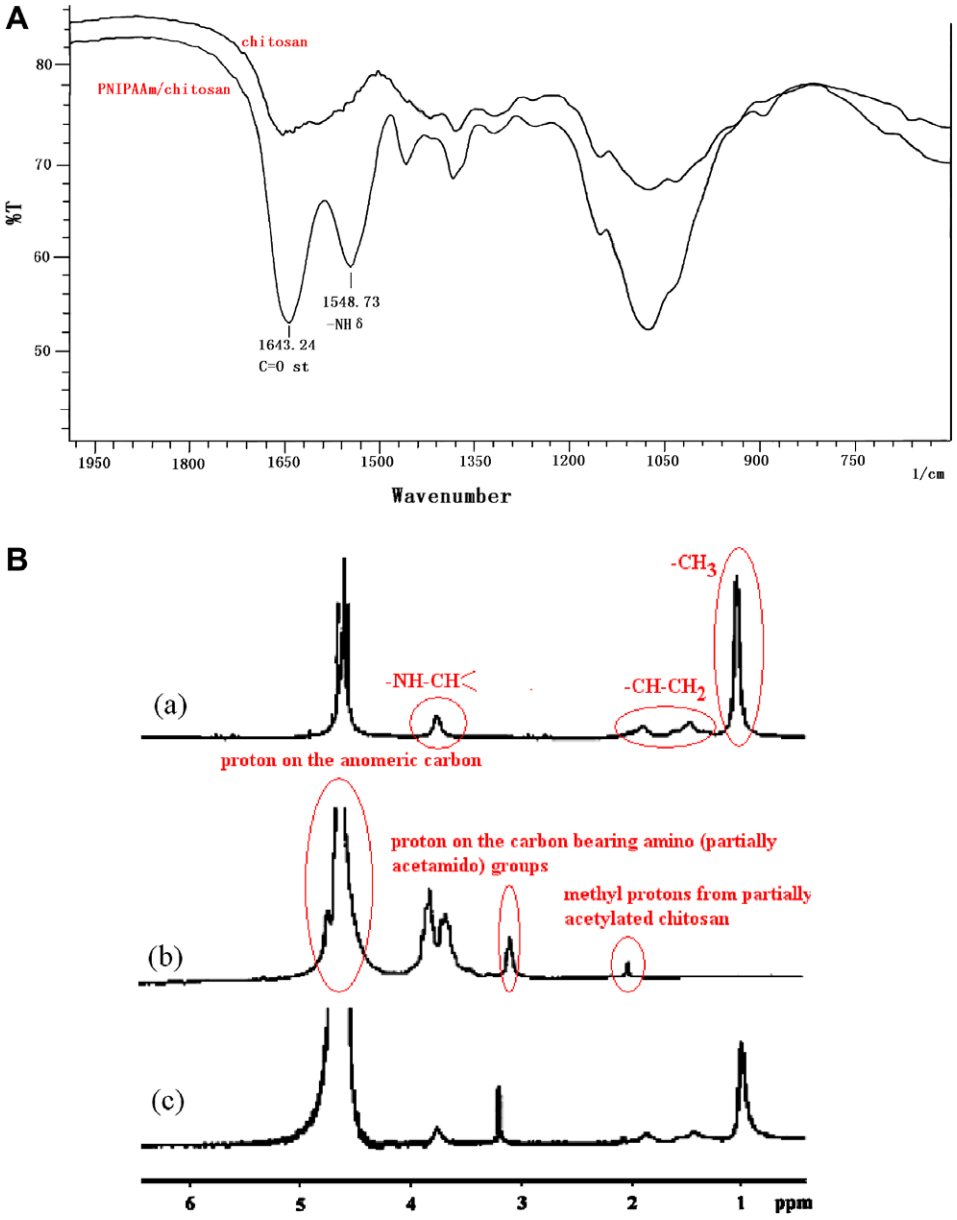

Fig. 1. (A) FTIR spectra of poly NIPAAm/chitosan nanoparticles in the comparison of chitosan. (B) ^{1}H-NMR spectra of poly NIPAAm/chitosan nanoparticles (c) in the comparison of PNIPAAm (a), chitosan (b).

nanoparticles with initially adding 50 mg of Rhodamine B isothiocyanate (RBITC) into the solution. The nanoparticles were collected by centrifugation and washed four times with distilled water. The dry nanoparticles were obtained by lyophilization and stored at 4 °C.

The analysis of interaction and internalization of RBITC-labeled nanoparticles were carried out on the cells grown on a 6-well plate. The RBITC-labeled nanoparticle-treated cells were washed three times with PBS at pH 6.8 and 7.4. The cells were then fixed with 95% ethanol for 30 min at room temperature. A cover slip was mounted on a glass microscope slide with a drop of glycerol as mounting medium. All specimens for the detection of RBITC were examined by a fluorescence microscope (Nikon H660L, Japan); the excitation and emission wavelengths were 540 and 580 nm, respectively.

3. Results and discussion

3.1. Characterizations of chitosan-g-NIPAAm

The poly NIPAAm/chitosan nanoparticles were prepared by the graft copolymerization of NIPAAm from chitosan in 70 °C aqueous media. TBHP first interacted with the amino groups on the polymer backbone to form amino and ^{t}BuO radicals. These radicals initiated the graft copolymerization of NIPAAm simultaneously with MBA as a cross-linker. The amphiphilic chitosan-g-PNIPAAm generated acted like surfactants, self-assembling to form nanoparticles with PNIPAAm as core and chitosan as shell. Percent of grafting is 711%. The PNIPAAm nanoparticles were prepared by the self-polymerization of NIPAAm monomer initiated by redox initiator. The chemical composition of both synthesized nanoparticles was confirmed by FTIR and ^{1}H NMR measurements. Incorporation of NIPAAm was confirmed by the formation of an extra peak at some wavelength. As shown in Fig. 1A, the typical carbonyl and amino group bands in amide at 1643 and 1548 cm^{-1}, respectively, were observed in the spectrum of synthesized nanoparticles. The strong evidence to confirm that NIPAAm was successfully incorporated into nanoparticles was that the characteristic bands of NIPAAm around 1540–1640 cm^{-1} appeared in the synthesized nanoparticles while it disappeared in chitosan.

^{1}H NMR spectroscopy measurements were carried out to identify the graft polymerization of NIPAAm onto chitosan. The spectrum of PNIPAAm (Fig. 1B-a) exhibited peaks (–CH–CH$_2$) at 100–2.00 ppm, a peak (–NH–CH<) at 3.79 ppm and a strong methyl group peak at 1.10 ppm. The peaks of vinyl protons (around 5.60–6.20 ppm) disappeared by the polymerization of NIPAAm. The spectrum of chitosan (Fig. 1B-b) exhibited typical peaks, including the proton on the anomeric carbon (at 4.65 ppm), the methyl protons from partially acetylated chitosan (at 1.99 ppm) and the proton on the carbon bearing amino (partially acetamido) groups (at 3.07 ppm). The spectrum of chitosan-g-NIPAAm copolymer in Fig. 1B-c is similar to that of PNIPAAm except a weak peak at 1.99 ppm and a proton peak at 3.07 ppm from the carbon bearing

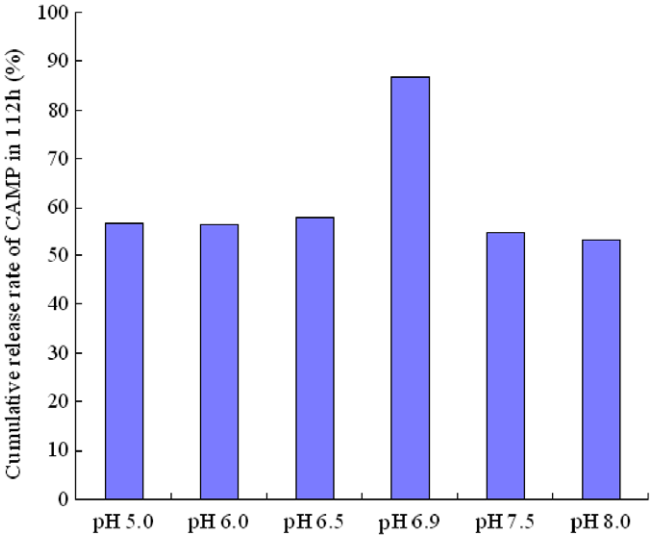

Fig. 3. Cumulative release rate of CAMP in various pH phosphate buffer at 36.5 ± 0.5 °C in 112 h.

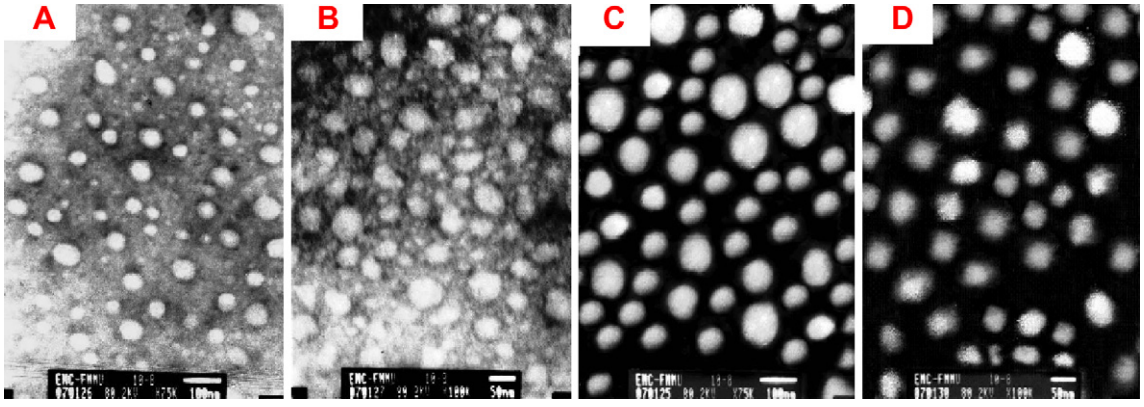

Fig. 2. TEM micrographs of PNIPAAm/chitosan nanoparticles (A); PNIPAAm nanoparticles (B); CAMP-loaded PNIPAAm/chitosan nanoparticles (C); CAMP-loaded PNIPAAm nanoparticles (D).

the amine (partially acetamido) groups of chitosan. It is estimated that the high content of PNIPAAm moiety was introduced to the chitosan backbone during the preparation of the water-soluble chitosan copolymer.

3.2. Drug loading level (LC%) and encapsulation efficiency (EE%) of CAMP-loaded PNIPAAm/chitosan nanoparticles

In this study, CAMP was successfully loaded into PNIPAM/chitosan nanoparticles by physically incorporating in the hydrophobic domains of the nanoparticles. The CAMP drug loading efficiency and encapsulation efficiency was 8.4% and 73.7%, respectively.

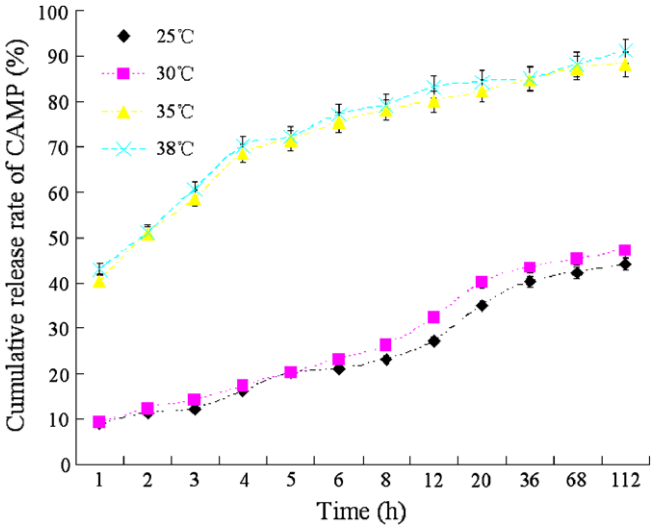

Fig. 4. Cumulative release rate of CAMP under various temperature in pH 6.5 phosphate buffer.

3.3. Morphology of the blank and drug-loaded nanoparticles

The morphology of the nanoparticles is an important consideration when evaluating the possibility of their use as carriers for targeted drug delivery. The blank nanoparticles (Fig. 2A and B) and drug-loaded nanoparticles (Fig. 2C and D) showed a spherical geometry and a uniform appearance by transmission electron microscope (TEM). The mean diameters of nanoparticles collected at 50–150 nm with favorable dispersibility.

3.4. In vitro release studies

Fig. 3 showed CAMP release profile in 112 h from CAMP-loaded poly NIPAAm/chitosan nanoparticles at various pHs (5.0, 6.0, 6.5, 6.9, 7.5, 8.0) at 36.5 ± 0.5 °C. Although the CAMP cumulative release rates from pH 5.0 to pH 6.0 were 22.32–30.03%, showing slight pH dependency, the cumulative release rates from pH 6.5 to pH 6.9 were 57.30–86.71%, showing drastically increased compared to that pH 5.0–6.0. As pH increased from 6.9 to 8.0, the cumulative release rate decreases from 86.71% to 54.16%, showing characteristic of reversible pH-response.

However, the release profile from drug loaded PNIPAAm nanoparticles did not show that pH-sensitive characteristic (data not shown).

In temperature-sensitive aspect, the tendencies of the drug release profiles in both poly NIPAAm/chitosan and PNIPAAm nanoparticles were similar. Fig. 4 showed

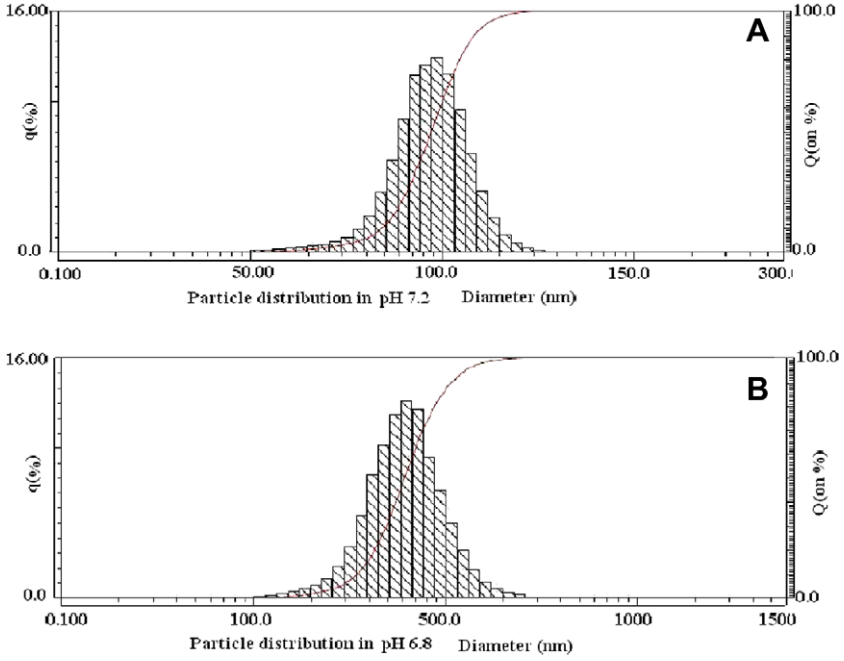

Fig. 5. Cumulative release rate of CAMP in physiological pH/temperature (pH 7.5, 36.8 °C) and in tumor extracellular pH/temperature (pH 6.8, 37.5 °C). The particle distribution in pH 7.2 (A) and in pH 6.8 (B).

cumulative release rate of CAMP under various temperature in pH 6.5 phosphate buffer in poly NIPAAm/chitosan nanoparticles. As the temperature increases from 25 to 40 °C, the cumulative release rate increases from 32.47% to 57.30%. Since the reaction was heated above the LCST of PNIPAAm, the PNIPAAm became hydrophobic during the polymerization. Above the LCST of PNIPAAm, the characteristic of hydrophobic increases with the increase of temperature. The cumulative release rate of CAMP in pH 6.5 increased from 25 to 40 °C because the hydrophobic degree of PNIPAAm increases along with the temperature increasing.

Fig. 5 showed the cumulative release rate differs from physiological conditions and tumor extracellular conditions in poly NIPAAm/chitosan nanoparticles. The cumulative release rate of CAMP was lower as 50.60% at physiological conditions while was much higher as 91.17% at tumor extracellular conditions. The expansion of chitosan shell and the minification of PNIPAAm core caused by the weak acidity and high temperature at tumor extracellular conditions, promote the release of CAMP all the more. However, the drug loaded PNIPAAm nanoparticles did not exhibit such characteristic (data not shown).

The mechanism research is under way. The process by phases indicated that in pH 7.2 the mean diameter of nanoparticles is smaller than 100 nm while in pH 6.8 it is nearly 480 nm (Fig. 5A and B). The swell of the nanoparticles is conspicuous in such small pH fluctuation. This result may provide evidence for the super pH sensitivity of CAMP release profile. It could be supposed that the intrinsic factor of POD release appears the characteristic of super pH sensitivity. At lower pH (about pH 6.8) and higher temperature (about 37.5 °C), the PNIPAAm core shrunk due to its hydrophobic interaction along with the

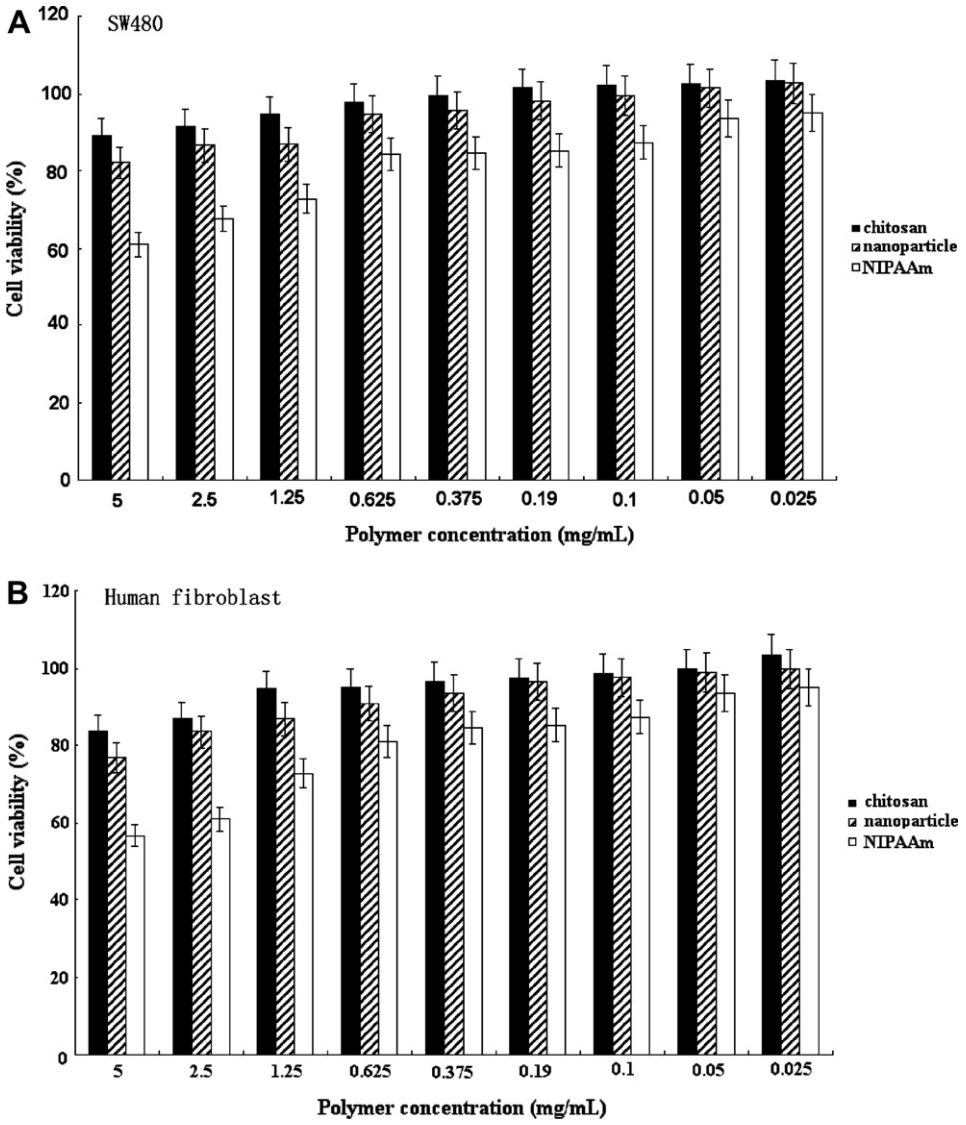

Fig. 6. Cytotoxicity of blank nanoparticles, chitosan and NIPAAm against human colon carcinoma cells SW480 (A) and human fibroblast (B) as a function of polymer/monomer concentration.

swell of the shell. This duplicate effect induced the enormous enhancement of drug release. Our further study results will hammer our point home with more evidences.

3.5. Stability of nanoparticles

The nanoparticles were stable with good fluidity when sealed and stored under common conditions, such as in a refrigerator or at room temperature for three months. Appearance of PNIPAMm/chitosan and PNIPAAm nanoparticles hardly occur any change.

3.6. In vitro cytotoxicity measurement of blank nanoparticles

MTT tests for blank nanoparticles showed that an increase in monomer/polymer concentration from 0.025 to 5 mg/mL was not harmful for the cell survival in human colon carcinoma cells SW480 and human fibroblast while compared with chitosan and NIPAAm (Fig. 6A and B). It was clear that a positive correlation found between cell cytotoxicity (MTT) and the concentration of NIPAAm monomers. Moreover, an obvious reduction in cell survival as the concentration increased above 1 mg/mL. For exam-

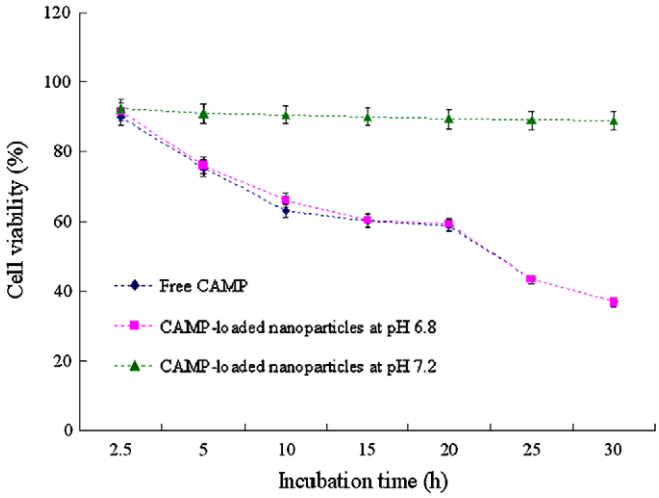

Fig. 8. Time-dependent cytotoxicity of drug-loaded nanoparticles compared to that of free CAMP against SW480 cells at pH 7.4 and pH 6.8 with a concentration of nanoparticles at 5.0×10^2 ng/mL.

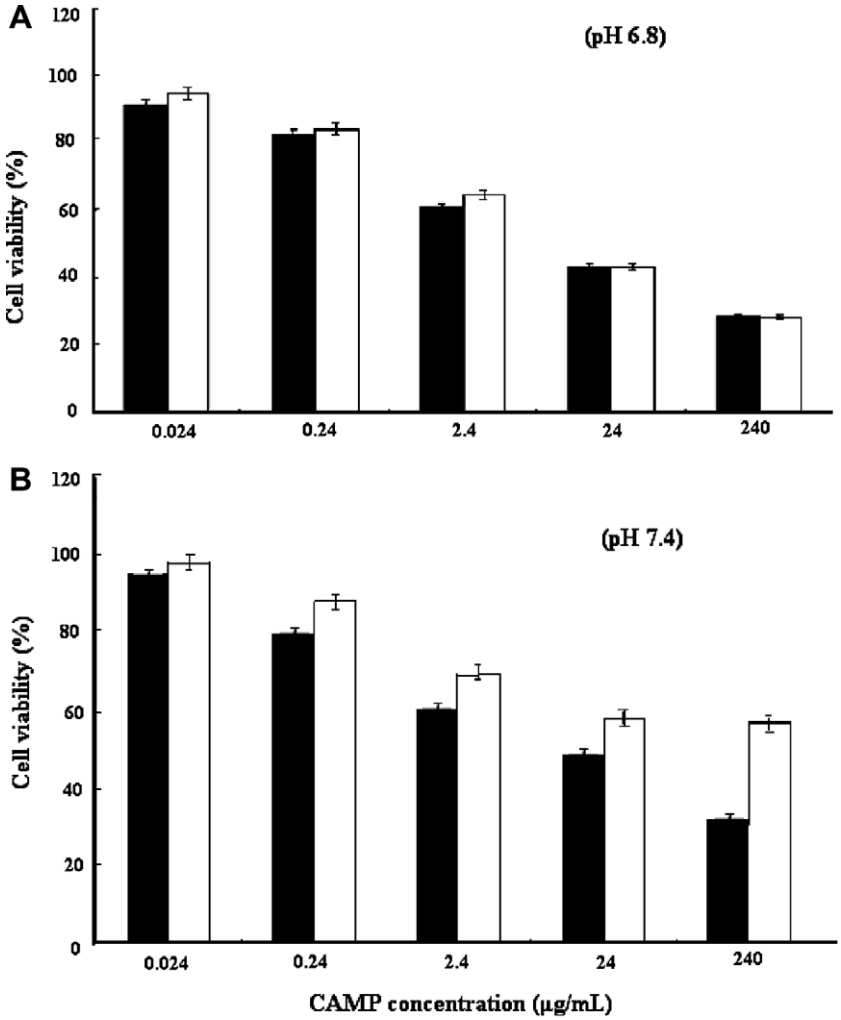

Fig. 7. Cytotoxicity of drug loaded nanoparticles compared with free CAMP against SW480 cells as a function of drug concentration at pH 6.8 (A) and pH 7.4 (B).

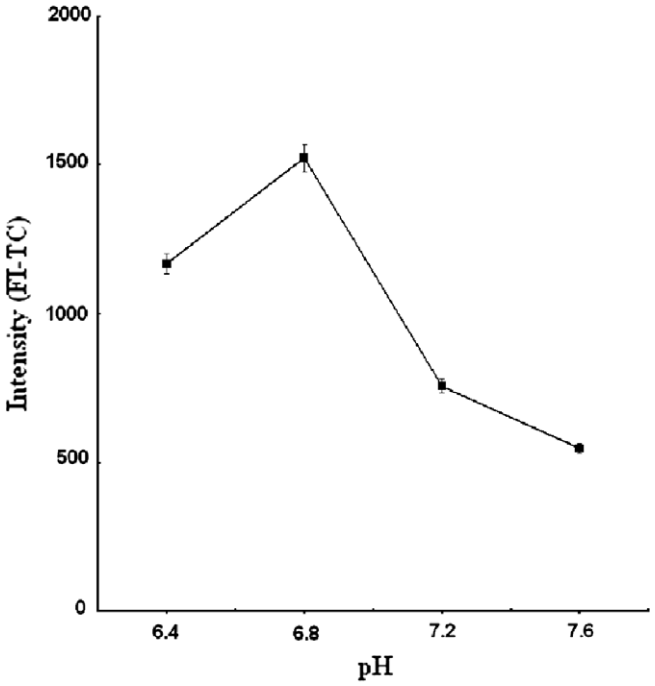

Fig. 9. The effect of pH on the interaction between nanoparticles and cells.

ple, the viability was only 58.5% in human fibroblast and 59.1% in human colon carcinoma cells SW480 at a concentration level of 5 mg/mL. However, conspicuous cytotoxicity of nanoparticles and chitosan was not found in the MTT test, and no remarkable cytotoxicity to the cells was observed after incubation. This result indicated that the biocompatibility of the nanoparticles was satisfactory.

3.7. pH-responsive cytotoxicity of drug loaded nanoparticles

The in vitro cytotoxicity to SW480 cells at pH 6.8 or 7.4 are compared with free CAMP as a control in Fig. 7A and B, respectively. At pH 7.4, there was no noticeable cytotoxicity of drug-loaded nanoparticles at the drug concentration range from 2.4×10^{-2} to 2.4×10^{2} μg/mL (Fig. 7B). However, at pH 6.8, drug-loaded nanoparticles showed significantly enhanced cytotoxicity (Fig. 7A).

The time course of drug loaded nanoparticles cytotoxicity at pH 6.8 and pH 7.4 was comparable with that of free CAMP (Fig. 8). The cytotoxicity of drug loaded nanoparticles in pH 6.8 and free CAMP during the time of 2.5–15 h sharply increased over time while drug loaded nanoparticles in pH 7.4 hardly presented cytotoxicity. This pronounced cytotoxicity of drug-loaded nanoparticles at pH 6.8 may attributed in part to the enhanced release rate of CAMP from the nanoparticles, and the total amount of released CAMP for 24 h was about 75% at pH 6.8 and about 35% at pH 7.4. The blank nanoparticles had hardly cytotoxicity, indicating that drug-free nanoparticles did not influence the viability of SW480 cells. Therefore, considering that the free drug added at the beginning to the cell culture, the enhanced cytotoxicity of drug-loaded nanoparticles does not rely entirely on the drug release rate, suggesting other factors for the observed cytotoxicity. Chung et al. reported that (Chung et al., 1999, 2000) the active interaction between polymeric micelles and the cells induced by hydrophobic PNIPAAm chains collapsed above LCST could provide high drug uptake by the cells through a more effective route. So the enhanced cytotoxicity of drug-loaded nanoparticles might due to two factors, super pH-sensitive drug release behavior and high drug uptake by the cells.

3.8. Observation of interaction between RBITC-labeled nanoparticle and SW480 cells

For a more detailed observation of the behavior of the nanoparticles with the cells, nanoparticles were labeled with RBITC as a fluorescence probe and the interaction with cells was monitored by fluorescence intensity

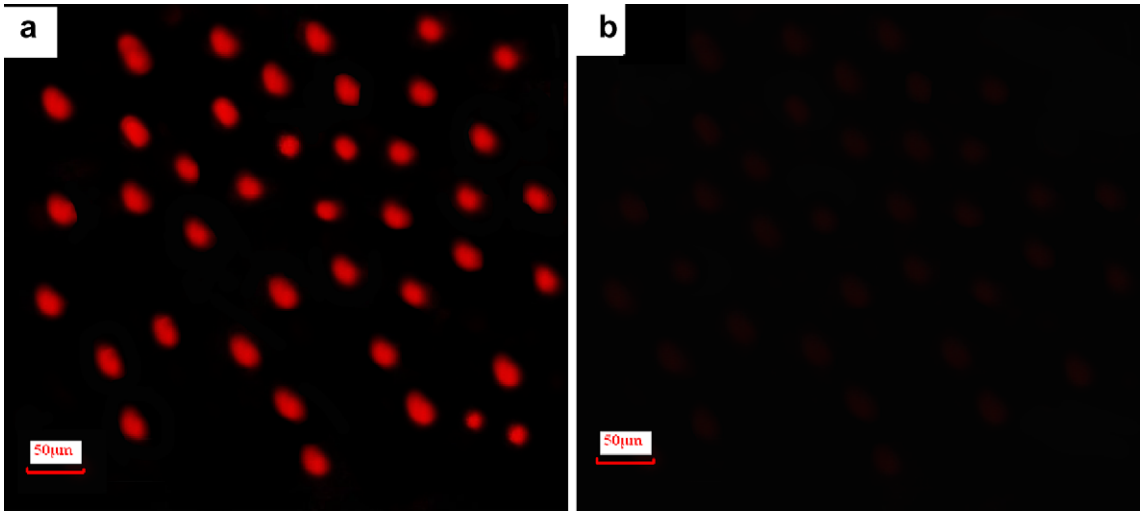

Fig. 10. Luminescence images of SW480 cells treated with RBITC-labeled nanoparticles at pH 6.8 (a), and 7.4 (b). The SW480 cells were incubated at 37 °C for 5 h.

measurement and fluorescence microscope. The blank RBITC-labeled nanoparticles were added to the SW480 cells culture medium. After each incubation pH or time, cells were washed with RPMI 1640 medium to remove unbound nanoparticles, and a microplate fluorescence reader determined fluorescence intensity on the cells. The effect of pH on the interaction between nanoparticles and cells was presented in Fig. 9.

Fluorescence microscopic study of SW480 cells was employed to visualize this interaction. At pH 7.4, SW480 cells hardly exhibited luminescence when incubated with RBITC-labeled nanoparticles while at pH 6.8, the luminescence images exhibited strong fluorescence (Fig. 10).

In a word, the results support that at pH 6.8, nanoparticles are being associated with the cells and internalized together with the entrapped drug in the cytoplasm, probably via endocytic mechanism. The improved interaction, intracellular localization and unidentified interactions of the nanoparticles at tumor pH, in addition to the accelerated release, led to the cytotoxicity comparable to that of the free drug.

4. Conclusions

Research efforts have been devoted to demonstrate in vitro that the pH-sensitive characteristic of poly NIPAAm/chitosan nanoparticles can be applied for targeting tumor cells. In that case, the CAMP loaded nanoparticles showed a drastically enhanced cytotoxicity compared to that at normal pH. Thereby, the atoxic poly NIPAAm/chitosan nanoparticles with an accelerated drug release at pH 6.8 compared to that of pH 7.4 has the potentiality as a novel anticarcinogen carrier. In summary, the super pH-sensitive nanoparticles show certain potential for drug delivery in specific sites such as tumor where local sites acidity and temperature has been developed. Advanced researches are ongoing to provide more evidences to confirm the fantastic possibility and feasibility for the novel super pH-sensitive drug carrier to target solid tumors punctually.

Acknowledgment

This study was supported by the grant of National Nature Science Foundation of China: No. 30300456 and No. 30770573.

References

Alvarez-Lorenzo, C., Concheiro, A., Dubovik, A. S., Grinberg, N. V., Burova, T. V., & Grinberg, V. Y. (2005). Temperature-sensitive chitosan-poly (*N*-isopropylacrylamide) interpenetrated networks with enhanced loading capacity and controlled release properties. *Journal of Controlled Release, 102*, 629–641.

Benrebouh, A., Avoce, D., & Zhu, X. X. (2001). Thermo- and pH-sensitive polymers containing cholic acid derivatives. *Polymer, 42*, 4031–4038.

Cai, H., Zhang, Z. P., Sun, P. C., He, B. L., & Zhu, X. X. (2005). Synthesis and characterization of thermo- and pH-sensitive hydrogels based on chitosan-grafted *N*-isopropylacrylamide via γ-radiation. *Radiation Physics and Chemistry, 74*, 26–30.

Cammas, S., Suzuki, K., Sone, C., Sakurai, Y., Kataoka, K., & Okano, T. (1997). Thermo-responsive polymer nanoparticles with a coreshell micelle structure as site-specific drug carriers. *Journal of Controlled Release, 48*, 157–164.

Cartier, S., Horbett, T. A., & Ratner, B. D. (1995). Glucose-sensitive membrane coated porous filters for control of hydraulic permeability and insulin delivery from a pressurized reservoir. *Journal of Membrane Science, 106*, 17–24.

Chiu, H. C., Wu, A. T., & Lin, Y. F. (2001). Synthesis and characterization of acrylic acid-containing dextran hydrogels. *Polymer, 42*, 1471–1479.

Chris, H. T., John, W., & Susan, G. A. (1998). Clinical applications of the camptothecins. *Biochimica et Biophysica Acta, 1400*, 107–119.

Chung, J. E., Yokoyama, M., & Okano, T. (2000). Inner core segment design for delivery control of thermo-responsive polymeric micelles. *Journal of Controlled Release, 65*, 93–103.

Chung, J. E., Yokoyama, M., Yamato, M., Aoyagi, T., Sakurai, Y., & Okano, T. (1999). Thermo-responsive drug delivery from polymeric micelles constructed using block copolymers of poly(*N*-isopropylacrylamide) and poly(butylmethacrylate). *Journal of Controlled Release, 62*, 115–127.

Conner, J., Yatvin, M. B., & Huang, L. (1984). pH-sensitive liposomes: Acid-induced liposomes fusion. *Proceedings of the National Academy of Sciences of the United States of America, 81*, 1715–1718.

Du, J., Dai, J., Liu, J. L., & Dankovich, T. (2006). Novel pH-sensitive polyelectrolyte carboxymethyl Konjac glucomannan-chitosan beads as drug carriers. *Reactive & Functional Polymers, 66*, 1055–1061.

Feil, H., Bae, Y. H., Feijen, J., & Kim, S. W. (1992). Mutual influence of pH and temperature on the swelling of ionizable and thermosensitive hydrogels. *Macromolecules, 25*, 5528–5530.

Kang, S. I., & Bae, Y. H. (2001). pH-Induced volume-phase transition by reversible crystal formation. *Macromolecules, 34*, 8173–8178.

Katayama, S., & Ohata, A. (1984). Reentrant phase transition in acrylamide-derivative copolymer gels. *Macromolecules, 17*, 2641–2643.

Kathmann, E. E. L., White, L. A., & McCormick, C. A. (1997). Electrolyte- and pH-responsive zwitterionic copolymers of 4-[(2-acrylamido-2-methylpropyl)-di-methylammonio]butanoate with 3-[(acrylamio-2-methyl-propyl)dimethylammonio]propanesulfonate. *Macromolecules, 30*, 5297–5304.

Kong, G., Braun, R. D., & Dewhirst, M. W. (2001). Characterization of the effect of hyperthermia on nanoparticle extravasation from tumor vasculature. *Cancer Res., 61*, 3027–3032.

Langerman, L., Chaimsky, G., Golomb, E., Tverskoy, M., Kook, A. I., & Benita, S. (1990). A rabbit model for evaluation of spinal anesthesia: Chronic cannulation of the subarachnoid space. *Anesthesia and Analgesia, 71*, 529–535.

Lin, C. L., Chiu, W. Y., & Lee, C. F. (2005a). Preparation of thermoresponsive core–shell copolymer latex with potential use in drug targeting. *Journal of Colloid and Interface Science, 290*, 397–405.

Lin, C. L., Chiu, W. Y., & Lee, C. F. (2005b). Thermal/pH-sensitive core-shell copolymer latex and its potential for targeting drug carrier application. *Polymer, 46*, 10092–10101.

Moertel, C. G., Schutt, A. J., Reitemeier, R. J., & Hahn, R. G. (1972). Phase II study of camptothecin (NSC-100880) in the treatment of advanced gastrointestinal cancer. *Cancer Chemotherapy Reports, 56*, 95–101.

Muggia, F. M., Creaven, P. J., Hansen, H. H., Cohen, M. H., & Sealwry, O. S. (1972). Phase I clinical trial of weekly and daily treatment with camptothecin (NSC-100880): Correlation with preclinical studies. *Cancer Chemotherapy Reports, 56*, 515–521.

Ogawa, Y., Ogawa, K., Wang, B. L., & Kokufuta, E. (2001). A biochemomechanical system consisting of polyampholyte gels with coimmobilized glucose oxidase and urease. *Langmuir, 17*, 2670–2674.

Philippova, O. E., Hourdet, D., Audebert, R., & Khokhlov, A. (1997). pH-responsive gels of hydrophobically modified poly-(acrylic acid). *Macromolecules, 30*, 8278–8285.

Sakata, M., Todokoro, M., Kai, T., Kunitake, M., & Hirayama, C. (2001). Effect of cationic polymer adsorbent pK on the selective removal of endotoxin from an albumin solution. *Chromatographia, 53*, 619–623.

Shu, X. Z., Zhu, K. J., & Song, W. H. (2001). Novel pH-sensitive citrate cross-linked chitosan film for drug controlled release. *International Journal of Pharmaceutics, 212*, 19–28.

Stubbs, M., McSheehy, P. M. J., Griffiths, J. R., & Bashford, C. L. (2000). Causes and consequences of tumor acidity and implications for treatment. *Molecular Medicine Today, 6*, 15–19.

Subrahmanyam, D., Renuka, B., Rao, C. V. L., Sagar, P. S., Deevi, D. S., Babu, J. M., et al. (1998). Novel D-ring analogues of CAMP as potent anti-cancer agents. *Bioorganic & Medicinal Chemistry, 8*, 1391–1396.

Suzuki, A., & Tanaka, T. (1990). Phase transition in polymer gels induced by visible light. *Nature, 346*, 345–347.

Tannock, I. F., & Rotin, D. (1989). Acid pH in tumors and its potential for therapeutic exploitation. *Cancer Research, 49*, 4373–4384.

Wang, M., Fang, Y., & Hu, D. (2001). Preparation and properties of chitosan-poly (*N*-isopropylacrylamide) full-IPN hydrogels. *Reactive & Functional Polymers, 48*, 215–221.

Yahara, T., Koga, T., Yoshida, S., Nakagawa, S., Deguchi, H., & Shirouzu, K. (2003). Relationship between microvessel density and thermographic hot areas in breast cancer. *Surgery Today, 33*, 243–248.

Yokoyama, M., & Okano, T. (1996). Targetable drug carriers: Present status and a future perspective. *Advanced Drug Delivery Reviews, 21*, 77–80.

Yuk, S. H., Cho, S. H., & Lee, S. H. (1997). pH/Temperature-responsive polymer composed of poly(N,N-dimethylamino)ethyl methacrylate-co-ethylacryamide. *Macromolecules, 30*, 6856–6859.